

1 **River deltas as Multiplex networks: A framework for studying multi-process**
2 **multi-scale connectivity via coupled-network theory**

3 Alejandro Tejedor¹, Anthony Longjas¹, Paola Passalacqua², Yamir Moreno^{3,4,5} and Efi Foufoula-
4 Georgiou^{1,6}

5 ¹ Department of Civil and Environmental Engineering, University of California, Irvine, Irvine, California, USA

6 ² Department of Civil, Architectural, and Environmental Engineering, Center for Water and the Environment, University of
7 Texas at Austin, Austin, Texas, USA

8 ³ Institute for Biocomputation and Physics of Complex Systems (BIFI), Universidad de Zaragoza, Zaragoza, Spain

9 ⁴ Departamento de Física Teórica, Universidad de Zaragoza, Zaragoza, Spain

10 ⁵ Institute for Scientific Interchange, ISI Foundation, Turin, Italy

11 ⁶ Department of Earth System Science, University of California, Irvine, Irvine, California, USA

12

13

14 **Abstract**

15 Transport of water, nutrients or energy fluxes in many natural or coupled human-natural systems
16 occurs along different pathways that often have a wide range of transport timescales and might
17 exchange fluxes with each other dynamically (e.g., surface-subsurface). Understanding this type
18 of transport is key to predicting how landscapes will change under changing forcing. Here, we
19 present a general framework for studying transport on a multi-scale coupled-connectivity system,
20 via a multilayer network, which conceptualizes the system as a set of interacting networks, each
21 arranged in a separate layer, and with interactions across layers acknowledged by interlayer
22 links. We illustrate this framework by examining transport in river deltas as a dynamic
23 interaction of flow within river channels and overland flow in the islands, when it is controlled
24 by the flooding level. We show the potential of the framework to answer quantitatively questions
25 related to the characteristic timescale of response in the system.

26 I. Introduction

27 Conceptualizing connectivity within a graph theoretic framework for studying processes
28 on the Earth's surface has seen increased interest over the last decades [e.g., see reviews -
29 *Phillips et al.*, 2015; *Heckmann et al.*, 2015; *Passalacqua*, 2017 - and references within]. In a
30 graph or network, nodes represent physical locations or state variables and links represent the
31 direction and strength of connectivity or interaction between nodes. In many physical systems,
32 transport takes place by more than one mechanisms, e.g., overland flow and channel flow, and
33 over different transport pathways, e.g., within the channel network and/or within the inter-
34 dispersed set of islands as overland flow, with exchange occurring between these two
35 interconnected systems depending on the magnitude of the system forcing and possibly local
36 conditions. To represent such a process within a network framework requires conceptualizing it
37 as a system of distinct networks, each with different transport properties, and with interaction
38 allowed between networks to accommodate the flux exchange. It is expected that considering the
39 overall system connectivity in this enlarged network perspective will result in emergent transport
40 properties and dynamics not possible to decipher by analyzing each network separately, and
41 therefore revealing key information essential to predict the system response under changing
42 forcing.

43

44 In recent years, a new framework that generalizes the traditional representation of
45 networks to the so-called multilayer networks was introduced [*Mucha et al.*, 2010; *De Dominicis*
46 *et al.*, 2013; *Boccaletti et al.*, 2014; *Kivela et al.*, 2014]. A multilayer network represents the
47 different connectivities arising from various processes as distinct networks (layers) but allows at
48 the same time to represent interactions between separate layers by introducing interlayer links

49 (across process interactions). The application of this framework has spanned diverse disciplines
50 ranging from social networks (e.g., propagation of information across different social media
51 platforms [Cozzo *et al.*, 2013]); to transportation networks (e.g., transportation in a multiplatform
52 system – subway and bus – [De Domenico *et al.*, 2014]) and biochemical networks (e.g.,
53 spreading of two diseases, which interact cooperatively [Sanz *et al.*, 2014]), to name a few.
54 Despite the enormous potential for the application of this framework to the study of diverse
55 surface or sub-surface processes, to the best of our knowledge it has not been utilized yet in the
56 earth sciences community. In this paper, we introduce this conceptual framework and illustrate it
57 in the case of transport in river deltas, demonstrating its potential to capture emergent overall
58 system behavior that arises from complex smaller-scale interactions.

59
60 River deltas are depositional landforms forming downstream of major rivers when
61 sediment-laden water slows down as it enters a body of standing water. Deltas contain nutrient-
62 rich sediments that support agriculture, they are rich in oil and hydrocarbon deposits, and provide
63 a variety of environmental services. However, many major deltas are losing land because of the
64 combined effects of (i) sediment deprivation due to dams and levees construction, (ii) accelerated
65 subsidence due to soil compaction exacerbated by groundwater and/or oil extraction, and (iii)
66 rising sea levels [Syvitski *et al.*, 2005; Ericson *et al.*, 2006; Blum and Roberts, 2009, Syvitski *et*
67 *al.*, 2009; Giosan *et al.*, 2014]. Deltas consist of a network of channels that tiles their surface
68 and that are surrounded by islands (inter channel areas) that are regularly inundated by river
69 flooding and tides. The channel networks transport water, solids (e.g., sediment) and solutes
70 (e.g., nutrients) across the delta top, maintain biotic and abiotic diversity, create islands that trap
71 sediment and enhance land building potential, provide corridors for the transport of goods and

72 services, and create an orderly arrangement of water-land patches that absorb or amplify external
73 perturbations. As such, substantial progress in understanding deltaic systems can be made by
74 studying the structure and function of their channel networks [*Smart and Moruzzi, 1971;*
75 *Morisawa 1985; Tejedor et al., 2015a,b; Tejedor et al., 2016; Tejedor et al., 2017*]. However, it
76 is well-known that water and sediment fluxes are not only confined to the delta channel network.
77 There are event-related, seasonal and permanent (e.g., close to the delta shoreline) water and
78 sediment exchanges between channels and islands. *Passalacqua* [2017] described this exchange
79 of fluxes between channels and islands in deltas as a “leaky network” of channels and islands.
80 For example, field measurements on the distal part of the Wax Lake delta in coastal Louisiana
81 show that around 23-54% of the water flux that flows into the feeder channel enter the islands
82 through secondary channels and subaqueous levees [*Hiatt and Passalacqua, 2015; 2017*].

83 Traditional single network approaches are not equipped to handle the connectivity
84 between the channel network (channelized flow) and islands (overland flow) for sediment and
85 water fluxes, with each network having different topologies and transport properties. In fact, the
86 channel–island *hydrological connectivity* in some cases can significantly affect the travel time
87 within the delta, due to the different timescales of transport occurring in the channels vs. the
88 islands. For example, by using tracer experiments in the distal part of the Wax Lake delta, *Hiatt*
89 *and Passalacqua* [2015] reported that the travel time through the islands can be three times
90 slower than its counterpart travel time through the channel network (channels ~ 4.4 hours;
91 islands ~ 14.3 hours). Also, the tracer particles can stay longer (~3.8 days) in the islands because
92 of the influence of tides and winds [*Hiatt and Passalacqua, 2015; Sendrowski and Passalacqua,*
93 2017].

94

95 In this paper, we present the mathematical framework required to integrate the different
96 connectivities into one mathematical object called multilayer network. In multilayer networks,
97 each layer consists of a distinct network, which characterizes the connectivity of a different
98 process acting on the system (e.g., for the channel-island dynamics in river deltas, one layer
99 accounts for the channel connectivity and another layer represents the connectivity that arises
100 from overland flow on islands). Since the processes occurring in each layer are not independent
101 of each other and across process interactions are expected, connectivity across layers is
102 accounted for by the existence of *interlayer connections* (e.g., acknowledging flux exchanges
103 between islands and channels).

104

105 **II. The mathematical framework: From single- to multi- layer connectivity**

106 *Tejedor et al.* [2015a] showed that a delta channel network connecting the delta apex to
107 the shoreline can be abstracted as a directed graph $G = (\mathcal{V}, \mathcal{E})$, defined as sets of N vertices $\mathcal{V} =$
108 $\{v_i\}, i=1, \dots, N$ (also called nodes), and E edges (or links) $\mathcal{E} = \{(uv)\}$, where $u, v \in \mathcal{V}$, and the
109 ordered pair (uv) denotes an edge starting at vertex u (parent) and ending at vertex v (child).
110 Specifically, for delta channel networks, the edges represent channels, and vertices correspond to
111 the locations where one channel splits into new channels (bifurcation), or where two or more
112 channels merge into a single channel (junction).

113

114 The connectivity structure of the delta graph can be uniquely specified by a binary square
115 $N \times N$ matrix called *Adjacency matrix* (A), whose entry a_{uv} is 1 if there exists a (vu) edge, that is a
116 channel from vertex v to vertex u ($a_{uv}=1$), and 0 otherwise. A more general version of the A
117 matrix is called the *Weighted Adjacency matrix*, W , where its entries w_{uv} are non-negative

118 numbers that quantify the strength of the connectivity between nodes v and u . For deltas, we
119 define w_{uv} as the fraction of the flux present at node v that flows through the channel (vu)
120 [Tejedor *et al.*, 2015a]. The advantage of this representation is that once all the connectivity
121 information is encoded in a matrix, by simple algebraic operations we can extract important
122 information on the structural patterns of the channel network (topology) as well as the steady
123 state flux distribution that emerges when the weights assigned to the edges are suitably chosen to
124 be representative of the flux partition at each bifurcation (e.g., proportional to channel widths).

125

126 From the Adjacency matrix alone, a different matrix called *Laplacian* L can be derived,
127 which is central for the analysis of many properties of graphs. Here, we define the Laplacian as
128 $L = S - W$, where S is the $N \times N$ diagonal matrix with diagonal entries $s_{vv} = \sum_{u=1}^N w_{uv}$, i.e., the
129 sum of the weights of all the edges leaving node v . Note that we denote here by L what is
130 generally known as the out-Laplacian [Tejedor *et al.*, 2015a].

131 The representation of multilayer networks requires a generalization of the previously
132 defined *Adjacency* and *Laplacian* matrices. Specifying the connectivity of traditional single-
133 layer networks (referred to herein as monoplex to indicate the special case of a multilayer
134 network with only one layer), only requires two indices per edge (parent and child node), which
135 makes matrices a suitable representation of networks. For multilayer networks two indices are
136 not enough, since we also need to specify the layers where each of the two nodes connected by
137 an edge belongs to. Tensors are the natural generalization of matrices when a higher
138 dimensionality is required (in fact matrices are tensors of second order – the order of a tensor can
139 be thought of as the number or indices needed to specify its entries). Consequently, we define

140 the multilayer Adjacency tensor \mathcal{M} whose entries $M_{uv}^{\alpha\beta}$ denote an edge starting at node v at layer
141 β and ending on node u in layer α [De Dominico et al., 2013].

142

143 There is a specific subclass of multilayer networks called multiplex networks (hereafter
144 referred to as multiplex) [De Dominico et al., 2013; Gomez et al., 2013; Tejedor et al., 2018],
145 wherein each layer consists of the same set of nodes but possibly different topologies (set of
146 edges) and layers interact with each other only via counterpart nodes in each layer (Fig. 1a). We
147 are especially interested in the multiplex because: (1) they are relevant to networks that are
148 embedded in space, where interactions across layers are not expected to happen between distant
149 nodes but only between counterpart nodes in the different layers (e.g., in deltas, the exchange of
150 fluxes between channels and islands occurs locally); (2) as we show below, the limitation of
151 having the interlayer connectivity only among counterpart nodes makes the mathematical
152 representation of multiplex simpler than for other multilayer networks.

153

154 Mathematically, a multiplex consisting of P layers, where each layer consists of a
155 network formed by the same set of N nodes, is described by a tensor $\mathcal{M} = \left[M_{uv}^{\alpha\beta} \right]_{u,v=1,\dots,N}^{\alpha,\beta=1,\dots,P}$. Note
156 that $M_{uv}^{\alpha\alpha}$ describes the Adjacency matrix of a monoplex in layer α , $A^{(\alpha)}$. Given the more
157 restrictive definition of multiplex, the entries corresponding to interlayer connectivity are defined
158 as follows: $M_{uv}^{\alpha\beta} = 0$ (different nodes u and v in different layers α and β), and $M_{uu}^{\alpha\beta} = 1$ (replica
159 nodes u in different layers α and β). The simple structure of the interlayer connectivity allows
160 us to project the Adjacency tensor in an $NP \times NP$ matrix, called *supra-Adjacency* matrix, \mathcal{A} . For
161 the case of two layers, \mathcal{A} takes the following form:

162

163

$$\mathcal{A} = \begin{pmatrix} A^{(C)} & I \\ I & A^{(I)} \end{pmatrix}, \quad (1)$$

164

165 where I is the $N \times N$ identity matrix. Here, we have used the notion $A^{(C)}$ and $A^{(I)}$, where the
 166 superscripts (C) and (I) denote channels and islands, respectively. Hence, the *supra-Adjacency*
 167 matrix is a block matrix, where each of the diagonal blocks encodes the intralayer connectivity of
 168 the respective layers, and the interlayer connectivity is stored in the off-diagonal blocks. Note
 169 that in \mathcal{A} replica nodes are labeled to satisfy $u+kN$ for $k=0,1, \dots, P-1$. The structure shown in Eq.
 170 1 (identity matrix for the off-diagonal blocks) guarantees that only across layer interactions
 171 between replica nodes are permitted.

172

173 Equivalently, a *supra-Laplacian* matrix \mathcal{L} can be defined for any multiplex. For the case
 174 of two layers, \mathcal{L} is defined as [Gomez *et al.*, 2013; Tejedor *et al.*, 2018]:

175

176

$$\mathcal{L} = \begin{pmatrix} D_C L^{(C)} + D_X I & -D_X I \\ -D_X I & D_I L^{(I)} + D_X I \end{pmatrix}, \quad (2)$$

177

178 where D_C is the intralayer diffusion coefficient in the channels, D_I the intralayer diffusion
 179 coefficient in the islands, D_X is the interlayer diffusion coefficient, and $L^{(C)}$ and $L^{(I)}$ are the out-
 180 Laplacian operators of the intralayer connectivity of the respective layers as defined for the
 181 monoplex. The nomenclature of the parameters D_C , D_I and D_X as diffusion coefficients is
 182 reminiscent of the interpretation of L as the diffusive operator in networks [Newman, 2010]. In a

183 more general setting, we can interpret those coefficients as scalars that allow to modify the
184 relative celerity of the process of each layer and the interlayer processes.

185

186 This framework allows us to formally formulate questions and provide quantitative
187 answers about the structural and dynamic connectivity of the integrated system. For instance, in
188 a river delta system, where the timescales of transport via channels or overland flow on islands
189 are significantly different, and where the flux exchange between these two transport mechanisms
190 depends on variables such as river discharge, it is interesting to ask under what conditions and
191 through which local interactions (exchanges) the overall system might exhibit accelerated
192 transport not expected by each system alone. Quantifying the system's timescales of response as
193 a function of the coupling (discharge) between layers and comparing this with the timescales of
194 the forcings (e.g., the timescale at which a given water discharge is exceeded) has important
195 implications for the understanding of many biogeomorphic processes (e.g., sediment trapping
196 and delivery of nutrients to the delta top).

197

198 **III. A Continuous Time Markov Chain (CTMC) as proxy for flux dynamics in river deltas**

199 We use a simple CTMC model to approximate the dynamics and relative timescales for
200 achieving steady state distributions when different values of coupling (flux exchange) are
201 assumed between the channel and island layers. The CTMC relies on several assumptions such
202 as: (i) a constant rate of transition, i.e., the partition of fluxes at a given bifurcation remains
203 constant and proportional to the physical parameters of the network, e.g., channel width; and (ii)
204 the Markovian property, i.e., the downstream direction that a given package of water or sediment
205 particles takes at a given bifurcation depends only on the physical properties of that bifurcation,

206 and not on the trajectory of the package in its journey from upstream. Despite these assumptions,
207 CTMC offers a good first-order approximation of the dynamics of the system.

208

209 The negative *supra-Laplacian* $-\mathcal{L}$ (see Eq. 2) can be interpreted as the transition-rate
210 matrix of the CTMC [Norris, 1997; Masuda et al., 2017]. The dynamics of the corresponding
211 Continuous Time Random Walk (CTRW) are governed by

212

$$\dot{\mathbf{p}}(t) = -\mathcal{L}\mathbf{p}(t), \quad (3)$$

214 where the i -th component of $\mathbf{p}(t)$ represents the probability that the CTRW visits node i at time t .

215

216 If the directed network is strongly connected, a unique stationary distribution of
217 probability \mathbf{p}_s , referred in the rest of the paper as steady state, exists [see Tejedor et al., 2018 for
218 further details]

219

$$\mathcal{L}\mathbf{p}_s = 0. \quad (4)$$

221 The rate of convergence towards the steady state given by \mathbf{p}_s is exponential
222 (asymptotically) with rate $\text{Re}(\lambda_2)$, where λ_2 is the eigenvalue with the smallest nonzero real part
223 [Lodato et al., 2007; Masuda et al., 2017; Tejedor et al., 2018]. Equivalently, the time of
224 convergence to steady state, τ , is inversely proportional to the rate of convergence ($\tau \propto$
225 $1/\text{Re}(\lambda_2)$). Note that the spectrum of eigenvalues of \mathcal{L} is in general complex since it is not
226 symmetric. Considering the definition of \mathcal{L} (see Eq. 2), its eigenvalue spectra, and more
227 specifically $\text{Re}(\lambda_2)$, depend on the following: (1) the topology of the connectivity of layer 1 – L_1 ,

228 (2) the diffusion coefficient of layer 1 - D_1 , (3) the topology of the connectivity of layer 2 - L_2 ,
229 (4) the diffusion coefficient of layer 2 - D_2 , and (5) the interlayer diffusion coefficient - D_X .

230

231 **IV. A multiplex case study: Wax Lake delta**

232 The Wax Lake delta is a river-dominated delta located in the coast of Louisiana, USA.
233 Sub-aerial land developed after the 1970s flood and the delta has been rapidly prograding ever
234 since [*Roberts et al.*, 1997; *Paola et al.*, 2011; *Shaw et al.*, 2013]. Lidar surveys have shown that
235 83% of the delta top experienced aggradation between 2009 and 2013 [*Wagner et al.*, 2017].
236 Primary channels transport water and sediment in the delta to the Atchafalaya Bay and secondary
237 channels connect the delta channel network to the island interiors [*Shaw et al.*, 2013].

238 Using the channel network connectivity of Wax Lake delta - channel layer (C) - together
239 with the island connectivity - island layer (I) - (see Fig. 1b and supplementary information for
240 further details about the connectivity used and a brief discussion of the deltaic system), we
241 examine the timescale of response of this coupled system. Without loss of generality, we have
242 set the value of $D_I = 1$. The value of $D_C = 7$ has been selected in order to generate rates of
243 convergence to steady state for the channel layer that are three times faster than those of the
244 islands, which are compatible with data collected from field campaigns (see *Hiatt and*
245 *Passalacqua* [2015] - channels ~ 4.4 hours; islands ~ 14.3 hours). The rate of water and
246 sediment exchange between the channels and islands is controlled by hydrologic (e.g., level of
247 water discharge) and eco-geomorphic (e.g., vegetation, existence of secondary channels
248 connecting the channel network to the interior of the islands) attributes. The effect of vegetation
249 is summarized into the value of D_I , i.e., more vegetated islands exhibit a higher roughness, and
250 therefore are expected to have a lower value of the diffusion coefficient D_I . Thus, the value of

251 D_X is mostly controlled by the discharge level, as here other forcings such as tides and wind are
252 ignored. Note that we assume that the value of D_X is homogeneous across the delta. This
253 assumption is an oversimplification given the existence of secondary channels in some of the
254 islands, gradients in vegetation and connectivity toward the distal part of the deltaic system, etc.
255 and therefore, a spatially explicit modulation of this parameter would make the model more
256 realistic. However, for the sake of simplicity in the presentation of the framework, we assume
257 uniform values of D_X , showing that even in this very simplified scenario, interesting and
258 unexpected system-wide behaviors emerge from the coupled dynamics. This simplification also
259 allows us to demonstrate that the system response described below does not emerge from
260 heterogeneity in the spatial patterns of D_X , but it is intrinsic to the coupled connectivity between
261 the channel and island layers.

262

263 By analyzing the behavior of the timescale of convergence of the channel-island system
264 to steady state, τ , as a function of the interlayer coupling, D_X , (Fig. 2a) the existence of four
265 regimes stands out: (1) *Linear*: The dynamics in the channel network and on the islands are
266 effectively decoupled wherein the rate of flux exchange between both layers (D_X) is the limiting
267 factor. In this regime, the timescale of convergence to steady state (τ) decreases linearly as $2D_X$.
268 (2) *Sublinear*: The coupling between channels and islands starts to be more significant but is
269 limited by the slower diffusion process in the islands. Here, an increase in D_X , i.e., a larger water
270 discharge, translates into a sublinear increase in the timescale of convergence to steady state for
271 the overall delta. (3) *Asymptotic*: For very large values of discharge (i.e., $D_X \gg \text{Re}(\lambda_2^I), \text{Re}(\lambda_2^C)$)
272 the two layers are completely coupled. This scenario can occur when the water discharge is
273 large enough to generate sheet flow on the whole system, where the counterpart nodes in the

274 different islands and channels are fully synchronized, behaving as single nodes. (4) *Prime*: This
275 regime, characteristic of multiplex with directed connectivity in at least one of its layers [Tejedor
276 *et al.*, 2018], occurs for intermediate values of coupling (discharge - D_X), wherein the rate of
277 convergence in the overall system achieves the shortest timescale, even shorter than in the
278 asymptotic regime. Physically, this regime can be interpreted as levels of discharge that produce
279 rates of channel-island flux exchange similar to the rates characteristic of channel transport
280 ($D_X \sim \text{Re}(\lambda_2^c)$). Thus, the islands and channels contribute significantly to the total transport but
281 conserving a relative degree of independence in their internal dynamics (i.e., not fully
282 synchronized or decoupled).

283

284 It is important to notice that although the parameter that controls the flux exchange
285 between the channel and island layers, D_X , is solely interpreted in terms of water discharge,
286 island roughness (e.g., due to vegetation) has been shown to effectively play a fundamental role
287 in the water exchange between islands and channels [Hiatt and Passalacqua, 2017]. The
288 multiplex framework allows us to easily assess the effect of different island roughness (mediated
289 by the value of D_I) in the system-wide response. When different scenarios of increasing island
290 roughness ($D_I = 1, 0.5$ and 0.1) are explored for a constant $D_C = 7$ (Fig. 2b), the transition from
291 the linear to the sublinear regime shifts to smaller values of D_X (discharge), acknowledging the
292 fact that the increased island roughness (i.e., lower value of D_I) makes the transport on islands
293 the limiting factor for a larger range of discharges. The immediate consequence of this shift in
294 the transition from linear to sublinear is that the system-wide response is significantly slowed
295 down for the same values of discharge under increased roughness scenarios. Finally, it is also
296 interesting to note the shift in the position of the minimum timescale of convergence to steady

297 state, τ , towards higher values of discharge (D_X) when higher values of island roughness (lower
298 values of D_I) are explored. Thus, for example, to achieve the shortest timescale of response of
299 the system in high roughness scenarios ($D_I = 0.1$), a 20% increase in the discharge (D_X) is
300 necessary when compared to the case of low roughness ($D_I = 1$).

301

302 Depending on the discharge levels (for given values of D_I and D_C), the delta multiplex
303 behaves as a channel-dominated system or a coupled channel-island complex. The geomorphic
304 (e.g., island aggradation) and biogeochemical (e.g., vegetation types, nutrient nourishment and
305 nitrogen fixation) consequences of operating in one or the other scenario are apparent. However,
306 to fully evaluate the overall system behavior, there are three relevant timescales associated with a
307 discharge Q (Fig. 3) that should be taken into consideration: t_d^Q - timescale associated with the
308 duration of the forcing; i.e., the time during which the value of Q is exceeded; t_r^Q - time of
309 recurrence of the forcing of magnitude Q ; and t_s^Q - timescale of response of the channel-island
310 delta system when both layers are coupled by a discharge level Q . The multiplex framework
311 allows to put into perspective these three timescales. Thus, the delta as a whole would be
312 efficient in redistributing sediments and nutrients, (i.e., it behaves as a channel-island complex),
313 if $t_s^Q \leq t_d^Q$, i.e., the time of response of the system is comparable with the duration of the forcing.
314 Thus, a deltaic system is resilient, i.e., it exhibits aggradation rates that are fast enough to self-
315 maintain the delta and the ecosystem services that it provides, if its overall delta connectivity has
316 evolved to a state wherein the prime regime of transport: (1) emerges for water discharge Q
317 (interlayer coupling) values with a recurrence time t_r^Q that is short enough to allow periodic

318 redistribution of fluxes at the delta scale and, (2) characterized by small values of t_S^0 (i.e.,
319 comparable in magnitude with the timescale of the transport in the channels).

320

321 **V. Conclusions and Perspectives**

322 To investigate transport properties of multi-process multi-scale connected systems we
323 introduce the framework of multilayer networks which allows to quantify properties of the
324 system as a whole, not accessible by studying each system separately. We illustrate this
325 framework by examining the flux dynamics in a river delta system, where channelized (within
326 the channel network) and overland (on the islands) flows are considered. We represent the delta
327 system as a two-layer multiplex, wherein each layer consists of the same number of nodes, but
328 the connectivity among them is different and representative of each process. The degree of
329 coupling among layers denotes the flux exchange in-between the two transport processes and is
330 mostly driven by the discharge level, although a strong control is also exerted by the relative
331 roughness of the islands (e.g., vegetation). To illustrate the potential of this framework, we
332 investigate the timescale of convergence to the steady state flux distribution for different degrees
333 of coupling, revealing the existence of four different regimes: linear, sublinear, prime and
334 asymptotic. We highlight that the prime regime, where the timescale of convergence to steady
335 state achieves its smallest value, occurs for intermediate values of coupling, i.e., not extreme
336 values of discharge, where the redistribution of sediment and nutrients is the fastest across the
337 delta top, enhancing the overall system aggradation and nourishment.

338

339 The application of this framework to specific systems in a more detailed manner opens up
340 interesting research questions such as (1) what is the return period of the discharge that

341 corresponds to the optimal coupling (1-year event, 10-year event, etc.) and how does it affect the
342 evolution of those systems and their resilience to extreme events, (2) what specific locations of a
343 delta might amplify across-process connectivity critically affecting the overall system transport
344 timescales; and (3) how is the system transport timescale dependent on including more or less
345 refined specification of across-process connectivity? For instance, by accounting for vegetation,
346 topography, etc., more layers can be included, with islands of similar characteristics (i.e., islands
347 that can be modeled by a similar diffusion coefficient) grouped in the same layer. Finally, we
348 want to emphasize the broad applicability of this framework to diverse fields in the geosciences
349 where multi-process multi-scale interactions dictate the overall system behavior. Examples
350 include flux transport taking into account surface-subsurface exchange [*Sawyer et al.*, 2015],
351 integrated wetland and river systems [*Hansen et al.*, 2017] and interaction types among species
352 in ecological systems [*Pilosof et al.*, 2017], etc.

353

354 **Acknowledgment**

355 This work is part of the International BF-DELTAS project on “Catalyzing action towards
356 sustainability of deltaic systems” funded by the Belmont Forum (NSF grant EAR-1342944) and
357 the LIFE (Linked Institutions for Future Earth, NSF grant EAR-1242458). Partial support is also
358 acknowledged from the Water Sustainability and Climate Program (NSF grant EAR-1209402).
359 A.T. acknowledges financial support from the National Center for Earth-surface Dynamics 2
360 postdoctoral fellowship (NSF grant EAR-1246761). Y. M. acknowledges partial support from
361 the Government of Aragón, Spain through a grant to the group FENOL, and by MINECO and
362 FEDER funds (grant FIS2014-55867-P). P. P. acknowledges support from the NSF grants:
363 CAREER/EAR -1350336, OCE-16002222 and EAR-1719670.

364 **References**

- 365 Blum, M. D., and H. H. Roberts (2009), Drowning of the Mississippi Delta due to insufficient
366 sediment supply and global sea-level rise, *Nat. Geosci.*, 2(7), 488–491.
367
- 368 Boccaletti, S., G. Bianconi, R. Criado, C. I. del Genio, J. Gómez-Gardeñes, M. Romance, I.
369 Sendiña-Nadal, Z. Wang, and M. Zanin (2014), The structure and dynamics of multilayer
370 networks, *Phys. Rep.*, 544(1), 1-122.
371
- 372 Cozzo, E., R. A. Baños, S. Meloni, and Y. Moreno (2013), Contact-based social contagion in
373 multiplex networks, *Phys. Rev. E*, 88, 050801(R).
- 374 De Domenico, M., A. Solé-Ribalta, E. Cozzo, M. Kivela, Y. Moreno, M. A. Porter, S. Gomez,
375 and A. Arenas (2013), Mathematical Formulation of Multilayer Networks, *Phys. Rev. X*, 3(4),
376 041022.
377
- 378 De Domenico, M., A. Solé-Ribalta, S. Gómez, and A. Arenas (2014), Navigability of
379 interconnected networks under random failures, *Proc. Natl. Acad. Sci.*, 111(23), 8351-8356.
380
- 381 Ericson, J.P., C. J. Vörösmarty, S. L. Dingman, L. G. Ward, and M. Meybeck (2006), Effective
382 sea-level rise and deltas: Causes of change and human dimension implications, *Global and*
383 *Planetary Change*, 50, 63–82.
384
- 385 Giosan, L., J. Syvitski, S. Constantinescu, and J. Day (2014), Climate change: protect the
386 world's deltas, *Nature*, 516, 31-33.
387
- 388 Gomez, S., A. Diaz-Guilera, J. Gomez-Gardeñes, C. J. Perez-Vicente, Y. Moreno, and A. Arenas
389 (2013), Diffusion Dynamics on Multiplex Networks, *Phys. Rev. Lett.*, 110(2), 028701.
390
- 391 Hansen, A. T., C. L. Dolph, E. Foufoula-Georgiou, and J. C. Finlay (2018), Contribution of
392 wetlands to nitrate removal at the watershed scale, *Nature Geoscience*, doi:10.1038/s41561-017-
393 0056-6.
394
- 395 Heckmann, T., W. Schwanghart, and J. D. Phillips (2015), Graph theory - recent developments
396 of its application in geomorphology, *Geomorphology*, 243, 130–146.
397
- 398 Hiatt, M., and P. Passalacqua (2015), Hydrological connectivity in river deltas: The first-order
399 importance of channel-island exchange, *Water Resour. Res.*, 51, 2264–2282,
400 doi:10.1002/2014WR016149.
401
- 402 Hiatt, M., and P. Passalacqua (2017), What controls the transition from confined to unconfined
403 flow? Analysis of hydraulics in a coastal river delta, *J. Hydraul. Eng.*, 143(6), 03117003.
404
- 405 Kivela, M., A. Arenas, M. Barthelemy, J. P. Gleeson, Y. Moreno, and M. A. Porter (2014),
406 Multilayer networks, *J. Complex Netw.*, 2(3), 203-271.
407

408 Lodato, I., S. Boccaletti, and V. Latora (2007), Synchronization properties of network motifs,
409 *Euro Phys. Lett.*, 78, 28001.

410 Masuda, N., M. A. Porter, and R. Lambiotte (2017), Random walks and diffusion on networks,
411 *Physics Reports*, 716-717, 1-58.

412
413 Morisawa, M. (1985), Topologic properties of delta distributary networks, in *Models in*
414 *Geomorphology*, edited by M. J. Woldenberg, pp. 239–268, Allen and Unwin, St. Leonards,
415 NSW, Australia.

416
417 Mucha, P. J., T. Richardson, K. Macon, M. A. Porter, and J.-P. Onnela (2010), Community
418 Structure in Time-Dependent, Multiscale, and Multiplex Networks, *Science*, 328 (5980), 876-
419 878, doi: 10.1126/science.1184819.

420
421 Newman, M. E. J. (2010), *Networks: An Introduction*, (Oxford University Press, New York).

422
423 Norris, J. R. (1997), *Markov Chains*, (Cambridge University Press, Cambridge, UK).

424
425 Paola, C., R. R. Twilley, D. A. Edmonds, W. Kim, D. Mohrig, G. Parker, E. Viparelli, and V. R.
426 Voller (2011), Natural Processes in Delta restoration: Application to the Mississippi Delta, *Annu.*
427 *Rev. Mar. Sci.*, 3, 67–91, doi:10.1146/annurev-marine-120709-142856.

428
429 Passalacqua, P. (2017), The Delta Connectome: A network-based framework for studying
430 connectivity in river deltas, *Geomorphology*, 277, 50–62, doi:10.1016/j.geomorph.2016.04.001.

431
432 Phillips, J. D., W. Schwanghart, and T. Heckmann (2015), Graph theory in the geosciences,
433 *Earth Sci. Rev.*, 143, 147–160.

434
435 Pilosof, S., M. A. Porter, M. Pascual and S. Kéfi (2017), The multilayer nature of ecological
436 networks, *Nat. Ecol. Evol.* 1, 0101.

437
438 Roberts, H. H., N. Walker, R. Cunningham, G. P. Kemp, and S. Majersky (1997), Evolution of
439 sedimentary architecture and surface morphology: Atchafalaya and Wax Lake Deltas, Louisiana
440 (1973–1994), *Trans. Gulf Coast Assoc. Geol. Soc.*, 47(42) 477–484.

441
442 Sanz, J., C.-Y. Xia, S. Meloni, and Y. Moreno (2014), Dynamics of Interacting Diseases, *Phys.*
443 *Rev. X*, 4(4), 041005, doi:10.1103/PhysRevX.4.041005.

444
445 Sawyer, A. H., D. A. Edmonds, and D. Knights (2015), Surface water- groundwater connectivity
446 in deltaic distributary channel networks, *Geophys. Res. Lett.*, 42, 10,299–10,306, doi:10.1002/
447 2015GL066156.

448
449 Sendrowski, A., and P. Passalacqua (2017), Process connectivity in a naturally prograding river
450 delta, *Water Resour. Res.*, 53, 1841–1863, doi:10.1002/2016WR019768.

451
452 Shaw, J. B., D. Mohrig, and S. K. Whitman (2013), The morphology and evolution of channels

453 on the Wax Lake Delta, Louisiana, USA, *J. Geophys. Res. Earth Surf.*, *118*, 1562–1584,
454 doi:10.1002/jgrf.20123.

455

456 Smart, J. S., and V. L. Moruzzi (1971), Quantitative properties of delta channel networks, *Tech.*
457 *Rep. 3*, 27 pp., IBM Thomas J. Watson Res. Cent., Yorktown, N. Y.

458

459 Syvitski, J. P. M., A. J. Kettner, A. Correggiari, and B. W. Nelson (2005), Distributary channels
460 and their impact on sediment dispersal, *Mar. Geol.*, *222–223*, 75–94.

461

462 Syvitski, J. P. M., et al. (2009), Sinking deltas due to human activities, *Nat. Geosci.*, *2*(10), 681–
463 686, doi:10.1038/ngeo629.

464

465 Tejedor, A., A. Longjas, I. Zaliapin, and E. Foufoula-Georgiou (2015a), Delta channel networks:
466 1. A graph-theoretic approach for studying connectivity and steady state transport on deltaic
467 surfaces, *Water Resour. Res.*, *51*, 3998-4018.

468

469 Tejedor, A., A. Longjas, I. Zaliapin, and E. Foufoula-Georgiou (2015b), Delta channel networks:
470 2. Metrics of topologic and dynamic complexity for delta comparison, physical inference, and
471 vulnerability assessment, *Water Resour. Res.*, *51*, 4019-4045.

472

473 Tejedor, A., A. Longjas, R. Caldwell, D. A. Edmonds, I. Zaliapin, and E. Foufoula-Georgiou
474 (2016), Quantifying the signature of sediment composition on the topologic and dynamic
475 complexity of river delta channel networks and inferences toward delta classification, *Geophys.*
476 *Res. Lett.*, *43*, 3280-3287.

477

478 Tejedor, A., A. Longjas, D. Edmonds, T. Georgiou, I. Zaliapin, A. Rinaldo, and E. Foufoula-
479 Georgiou (2017), Entropy and optimality in river deltas, *Proc. Natl. Acad. Sci., USA*, *114*(44),
480 11651-11656.

481

482 Tejedor, A., A. Longjas, E. Foufoula-Georgiou, T. Georgiou, and Y. Moreno (2018), Diffusion
483 Dynamics and Optimal Coupling in Directed Multiplex Networks, Under Review, *Physical*
484 *Review X*.

485

486 Wagner, W., D. Lague, D. Mohrig, P. Passalacqua, J. Shaw, and K. Moffett (2017), Elevation
487 change and stability on a prograding delta, *Geophys. Res. Lett.*, *44*, 1786–1794, doi:10.1002/
488 2016GL072070.

489

490

491

492

493

494

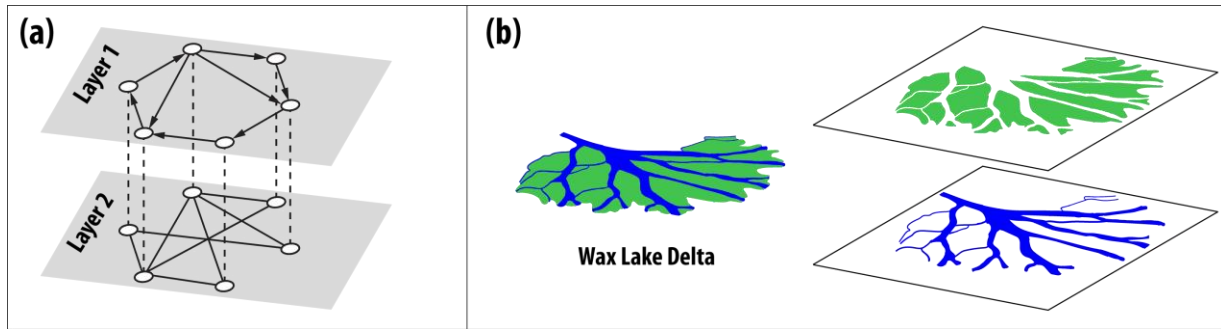
495

496

497

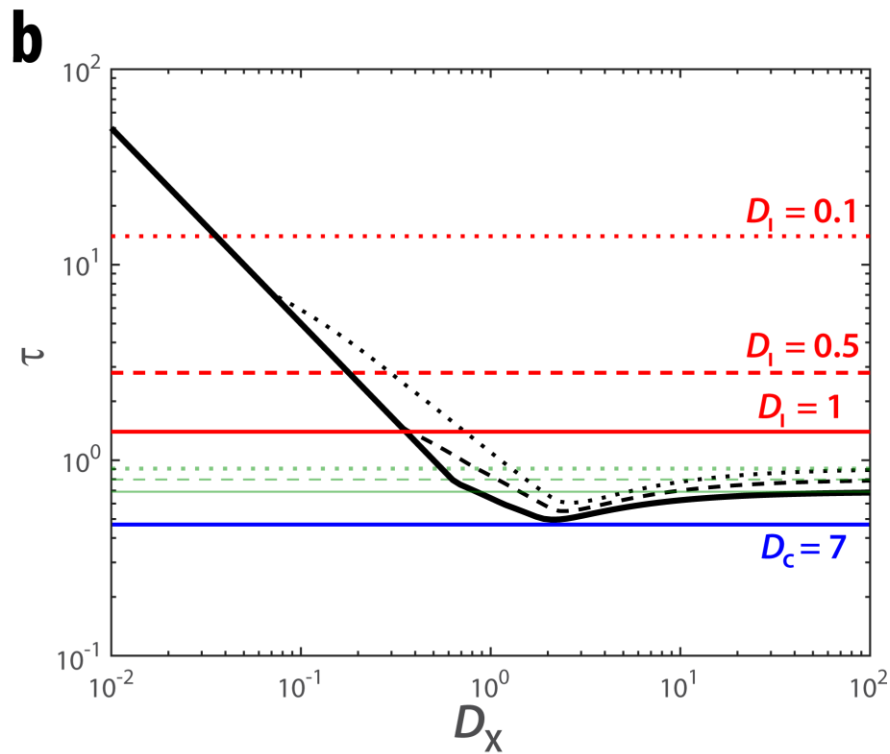
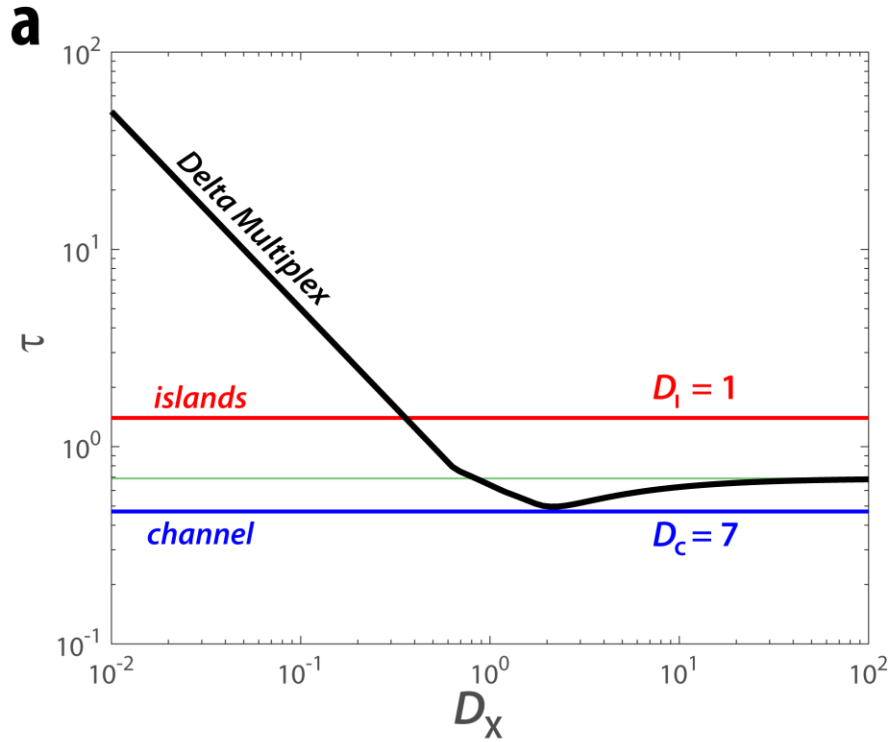
498

500



501 **Figure 1. Delta Multiplex (a)** *Illustration of a multiplex:* Multiplex are coupled multilayer
 502 networks where each layer consists of the same set of nodes but possibly different topologies (set
 503 of links) and layers interact with each other only via replica nodes in each layer (dashed lines)
 504 **(b)** *Wax Lake Delta Multiplex.* Illustration of the Wax Lake delta in the Louisiana coast (USA).
 505 The delta multiplex consists of two layers: Layer 1 (Bottom) accounts for the channel
 506 connectivity, and Layer 2 (Top) represents the connectivity that arises from overland flow on
 507 islands. For more details about the multiplex structure see supplementary materials.

508



509

510 **Figure 2. Flux Dynamics on the Wax Lake Delta Multiplex.** We show for the Wax Lake
 511 multiplex, the timescale of convergence to steady state, τ , as a function of interlayer coupling,

512 D_X , which is mostly controlled by water discharge. Panel (a) shows the emergence of a non-
513 monotonic behavior of τ as function of D_X , when the values of diffusivity of each layer are set to
514 $(D_C, D_I)=(7, 1)$ to reproduce the ratio of timescales of transport channel to island reported from
515 field campaigns. Panel (b) shows the effect of island roughness in the response timescale of the
516 delta multiplex. For intermediate values of D_X , the timescale of the delta multiplex τ decreases
517 for higher island roughness - $D_I= 1$ (solid lines), 0.5 (dashed lines) and 0.1 (dotted lines) -
518 reducing effectively the coupling between the channels and islands for the same values of D_X .

519

520

521

522

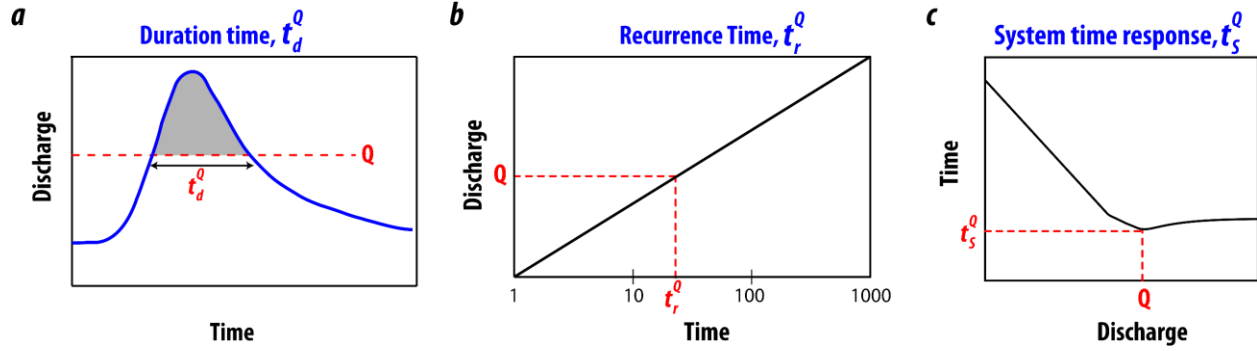
523

524

525

526

527



528

529 **Figure 3. The timescales associated with discharge Q .** (a) t_d^Q - timescale associated with the
 530 duration of the forcing; i.e., the time during which the value of Q is exceeded; (b) t_r^Q - time of
 531 recurrence of the forcing of magnitude Q ; and (c) t_s^Q - timescale of response of the channel-
 532 island delta system (see Fig. 2) when both layers are coupled by a discharge level Q .

533

534

535

536

537

538

539

540

541

542

543

544

545

546

547 **Supplementary Information**

548 **Description of the delta multiplex**

549 The Wax Lake multiplex delta consists of two layers: one layer accounts for the Delta
550 Channel Network (DCN) and another layer represents the connectivity that arises from overland
551 flow on islands – Delta Island Network (DIN). The connectivity across layers is accounted for
552 by the existence of *interlayer connections*, acknowledging flux exchanges between islands and
553 channels (see Fig. 1 in main text).

554

555 *Delta Channel Network (DCN)*

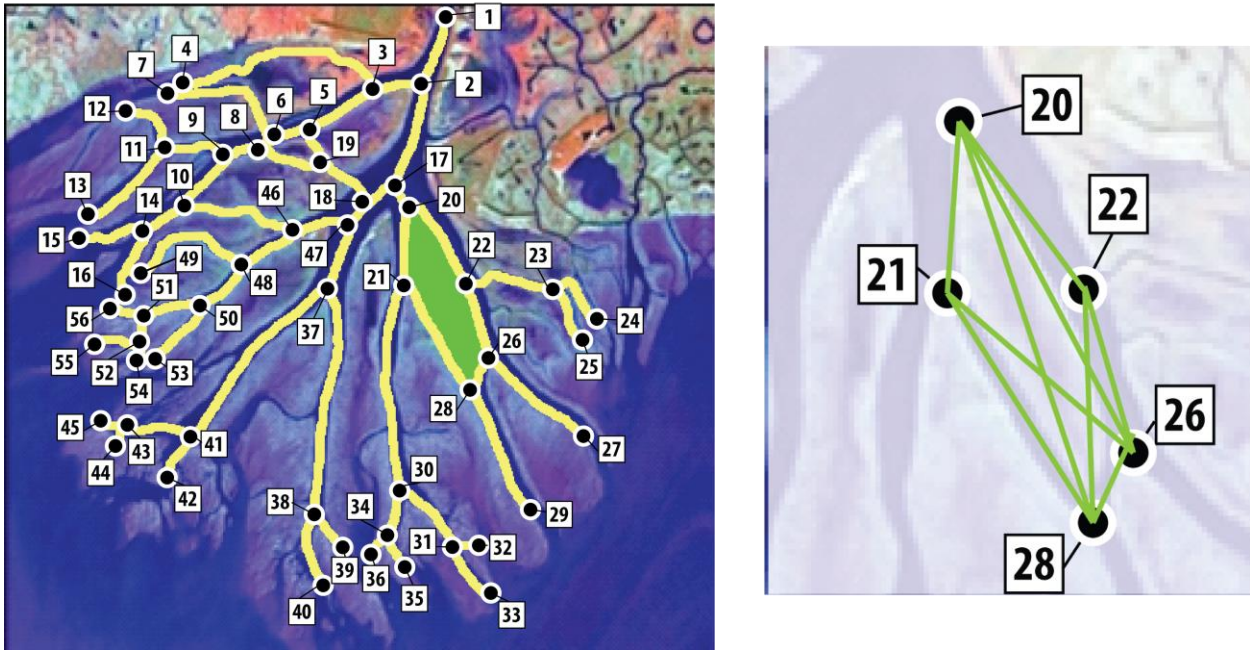
556 We utilized the outline of the Wax Lake delta structure processed by *Edmonds et al.*
557 [2011] and identified 56 nodes and 59 links (Figure S1 – left panel). All the information about
558 the connectivity (including directionality of the links) and the relative widths of the channels of
559 the DCN is stored in the Weighted Adjacency matrix, W^C , which is attached as a file
560 “WeightedAdjacencyMatrixDCN.dat” in the Supplementary Materials.

561 *Delta Island Network (DIN)*

562 The DIN consists of the same set of nodes in the DCN (56 nodes) but has different links.
563 An example of the DIN on one of the islands is shown in Fig. S1 (right panel). The links of the
564 DIN are directed and oriented in the downstream direction. The weights were computed
565 assuming that the strength of the connectivity is inversely proportional to the linear distance
566 between nodes within an island. The Weighted Adjacency matrix for the DIN, W^I , is attached as
567 a file “WeightedAdjacencyMatrixDIN.dat” in the Supplementary Materials. The entries, w_{uv} , of
568 the W^I are non-negative numbers and quantify the strength of the connectivity between nodes v
569 and u . For the DIN, w_{uv} accounts for the fraction of the flux present at node v that flows on the

570 island (overland flow) to node u .

571 Interlayer links only exist between counterpart nodes in the DCN and DIN.



572

573 **Figure S1. Wax Lake Multiplex Network.** Wax Lake delta in the Louisiana coast. **(Left**
574 **panel)** Delta Channel Network (DCN): The DCN (nodes as black circles and links as yellow
575 lines) is superimposed on the aerial view of the delta (photo obtained in 2005 by the National
576 Center of Earth-surface Dynamics, NCED). **(Right panel)** Delta Island Network (DIN): The
577 DIN is displayed for one of the islands (island colored in green in the left panel). The islands
578 network consists of the same set of nodes in the DCN, but the set of links (e.g., green lines) is
579 different.

580

581 **References:**

582 Edmonds, D. A., C. Paola, D. C. J. D. Hoyal, and B. A. Sheets (2011), Quantitative metrics that
583 describe river deltas and their channel networks, *J. Geophys. Res.*, *116*, F04022,
584 doi:10.1029/2010JF001955.